Applied Catalysis B: Environmental 189 (2016) 210–218

Contents lists available at ScienceDirect

Applied Catalysis B: Environmental

journal homepage: www.elsevier.com/locate/apcatb

Catalytic decomposition of gaseous ozone over manganese dioxides with different crystal structures

Jingbo Jia[a,b], Pengyi Zhang[a,b,*], Long Chen[c]

[a] State Key Joint Laboratory of Environment Simulation and Pollution Control, School of Environment, Tsinghua University, Beijing 100084, China
[b] Collaborative Innovation Center for Regional Environmental Quality, China
[c] The State Key Laboratory for Advanced Metals and Materials, University of Science and Technology Beijing, Beijing 100083, China

ARTICLE INFO

Article history:
Received 13 November 2015
Received in revised form 20 January 2016
Accepted 24 February 2016
Available online 27 February 2016

Keywords:
Manganese dioxide
Crystal structure
Ozone decomposition
Raman spectroscopy
Peroxide

ABSTRACT

Ozone is a ubiquitous pollutant and manganese dioxide (MnO_2) has been widely used for ozone decomposition. However, the effect of MnO_2 structure on ozone decomposition has never been investigated. Three tunnel-structure polymorphs, i.e., α-, β- and γ-MnO_2 were prepared and characterized by BET, TEM, XRD, H_2-TPR, O_2-TPD, NH_3-TPD, TGA-MS and XPS. The activity of three MnO_2 polymorphs for ozone decomposition followed the order of α- > γ- > β-MnO_2. The α-MnO_2 owned the largest specific surface area and lowest average oxidation state of Mn. Furthermore, the adsorbed oxygen species on the surface of α-MnO_2 were more easily reduced. In-situ Raman spectroscopy results showed that peroxide species formed during ozone decomposition, and over α-MnO_2 they were more easily decomposed by increasing reaction temperature. It was found that the catalytic activity of MnO_2 strongly depended on the density of oxygen vacancies. Accordingly, the ozone decomposition mechanism based on the involvement and recycling of oxygen vacancy (V_O) is proposed. The decomposition of peroxide species is a rate-limiting step. These findings are helpful for designing more effective catalyst for ozone removal.

© 2016 Elsevier B.V. All rights reserved.

1. Introduction

Tropospheric ozone is a secondary air pollutant formed via the photochemical reactions of anthropogenic primary pollutants involving nitrogen oxides (NO_x) and volatile organic compounds (VOCs) driven by sunlight [1]. Exposure to high concentration ozone causes detrimental effect on human health including pulmonary function and airway inflammation [2], blood pressure [3], premature mortality [4], and reduces yields of staple crops [5]. Moreover, tropospheric ozone itself acts as a greenhouse gas and therefore contributes to global warming [6].

Most people spend the majority of their time indoors, so much of their exposure to ozone actually occurs inside buildings. The dominant source of indoor ozone is ambient ozone that penetrates indoors [7]. Besides, several kinds of indoor equipment involved high voltage discharge, electrostatic discharge or ultraviolet light irradiation (such as photocopiers, air-condition, sterilizer, etc.) contribute to elevated indoor ozone levels. Several investigations have shown that indoor ozone can trigger secondary reactions and some known byproducts of these reactions include formaldehyde, organic acids and ultrafine particles [8–11]. Besides, catalytic ozonation is widely employed in low-temperature oxidation of volatile organic compounds (VOCs) in gas phase especially at low levels [12–19]. Usually the concentration of ozone in the off-gas from the process is well above the allowable values.

Catalytic materials explored for eliminating O_3 include noble-metal [20], various transition metal oxides supported on Al_2O_3 [21–23], SiO_2, TiO_2, activated carbon [24–28], cordierite [29] and zeolite [19,30–32]. Among them, manganese oxides especially MnO_2 is most frequently studied. Oyama and co-workers [33,34] examined the effect of supports on the ozone decomposition activity and found that difference in the structure of the manganese active center was the origin of support effect on the activity. However, XRD analysis indicated that supported manganese oxide was a well dispersed species when the MnO_2 loading was low and the information on the crystal structure was not given [28]. Raman spectra merely indicated that the component of manganese oxide catalysts was one or more of Mn_3O_4, MnO_2, Mn_2O_3 and MnO_2 [22,27,33]. Therefore the relationship between structure of manganese oxides and their catalytic property for ozone decomposition is not clear. Only a few work have investigated the activity of manganese dioxides with specific crystal phase [35,36].

* Corresponding author at: State Key Joint Laboratory of Environment Simulation and Pollution Control, School of Environment, Tsinghua University, Beijing 100084, China.
E-mail address: zpy@tsinghua.edu.cn (P. Zhang).

http://dx.doi.org/10.1016/j.apcatb.2016.02.055
0926-3373/© 2016 Elsevier B.V. All rights reserved.

To learn the effect of crystal structure of MnO_2 on their activity for ozone decomposition and the essential influencing factors, three tunnel-structure polymorphs of MnO_2, i.e., α, β and γ-MnO_2 were prepared and tested for ozone decomposition in this study. It was found that α-MnO_2 had the highest activity, and the structure, morphology and redox properties of catalysts were characterized to illustrate the key factors influencing the ozone decomposition.

2. Experimental

2.1. Preparation of MnO_2 polymorphs

All chemicals were of analytical grade. α-, β- and γ-MnO_2 were synthesized by hydrothermal method as described in the literature [37]. Briefly, α-MnO_2 was synthesized by the hydrothermal reaction between $KMnO_4$ and $Mn(Ac)_2$ at 140 °C for 2 h β-MnO_2 and γ-MnO_2 were prepared via the hydrothermal reaction between $(NH_4)_2S_2O_8$ and $MnSO_4{\cdot}H_2O$ at 140 °C for 12 h, and at 90 °C for 24 h, respectively.

After the hydrothermal reaction, the resultant precipitates were filtered, washed and dried at 85 °C in air for 12 h. All the samples were compressed, crushed and sieved through 40–60 mesh sieves before the activity evaluation.

2.2. Characterization

The crystal structure of as-prepared samples was verified by X-ray diffractometer (XRD, O8 discover, Siemens) equipped with Cu Kα radiation at accelerating voltage and current of 40 kV and 40 mA, respectively. The specific surface areas of the catalysts were determined from N_2 adsorption/desorption analysis at 77 K with a QuadraSorb SI (Quantachrome). The samples were first degassed at 300 °C for 4 h before measurement. The specific surface areas were determined by BET equation in 0.09–0.3 partial pressure range.

The morphology was observed with FE-SEM (S-5500, Hitachi) and HRTEM (Tecnai G2 F30 S-TWIN). The chemical state of Mn and O was determined by X-ray photoelectron spectroscopy (XPS, Thermo ESCALAB250xi). TGA was performed with STA 449 F3 Jupiter® (NETZSCH) at a heating rate of 10 °C/min from 50 °C to 950 °C and the evolved gas was analyzed by mass spectrometry (QMS 403C, NETZSCH).

H_2-TPR profiles were recorded with AutoChemII 2920 (Micromeritics). 40 mg sample was placed in U-shaped quartz tube, heated to 105 °C and purged with helium gas (He) for 0.5 h and then reduced in the stream of a mixture of 5% H_2/Ar (50 mL/min) at a heating rate of 5 °C/min to 600 °C. The H_2 consumption was monitored by a thermal conductivity detector (TCD). For O_2-TPD analysis, 80 mg sample was placed in U-shaped quartz tube, heated to 105 °C and purged with He for 0.5 h to remove surface H_2O. After that, the catalyst was purged with a mixture of O_2/He (50/10 mL/min) at 25 °C for 0.5 h. Desorption of O_2 was carried out from 25 °C to 950 °C at a heating rate of 5 °C/min purged with He. For NH_3-TPD analysis, 100 mg catalyst was placed in U-shaped quartz tube, heated to 300 °C and then purged with He for 1 h. After that, the catalyst was purged with 10% NH_3/He for 0.5 h at 100 °C. Desorption of NH_3 was carried out from 100 °C to 450 °C at a heating rate of 10 °C/min in He, and then the temperature was maintained at 450 °C for 1 h to achieve complete desorption.

2.3. Catalytic activity test

The activity of as-synthesized samples for ozone decomposition was carried out in a flow-through quartz tube reactor (ϕ 6 mm) using 0.1 g of catalyst with size of 40–60 mesh at different temperatures and relative humidity ~1%. O_3 was generated by passing filtered clean air through a low-pressure mercury ultraviolet lamp (10 V/3 W, Guangdong cnlight technology company). The total flow rate through the reactor was maintained at 1.1 L/min using mass-flow meters and included ~14 ppm O_3 balanced with clean air. The ozone concentration was determined with an ozone analyzer (Model 49i, Thermo Scientific, USA). The weight space velocity was set at 660 L g^{-1} h^{-1}. The conversion was calculated from the proportion of inlet and outlet concentrations of ozone after 2 h reaction.

2.4. Ozone decomposition intermediates analysis

In-situ Raman spectroscopy was used to directly observe and identify intermediates during ozone decomposition. The in situ Raman spectra was recorded on a Renishaw inVia Raman Microscope with resolution of 2 cm^{-1}. The excitation source was an argon–ion laser at the wavelength of 532 nm. The CCR1000 catalyst cell reactor system (Linkam scientific instruments) was used to obtain continuous Raman spectrum under controlled temperature and flow rate of reactant stream. The catalyst of ~60 mg was pressed into thin wafer and mounted on a virtually unreactive disposable ceramic fabric filters placed inside the ceramic heating element. The temperature was accurately controlled by the T95 controller via the S-type platinum/rhodium thermocouple. The ozone was generated by passing pure oxygen through an electric field discharge ozone generator (Tonglin Technology) and the inlet ozone concentration was about 800 ppm. Spectra was acquired under oxygen flow and under ozone/oxygen mixture flow at different temperature.

3. Results and discussion

3.1. Crystal structure and textural properties

Fig. 1 shows the XRD patterns of as-prepared catalysts, which correspond well to α-MnO_2 (JCPDS 44-0141), β-MnO_2 (JCPDS 24-0735) and γ-MnO_2 (JCPDS 17-0510), respectively. The XRD patters indicate that as-prepared catalysts are well crystallized and no

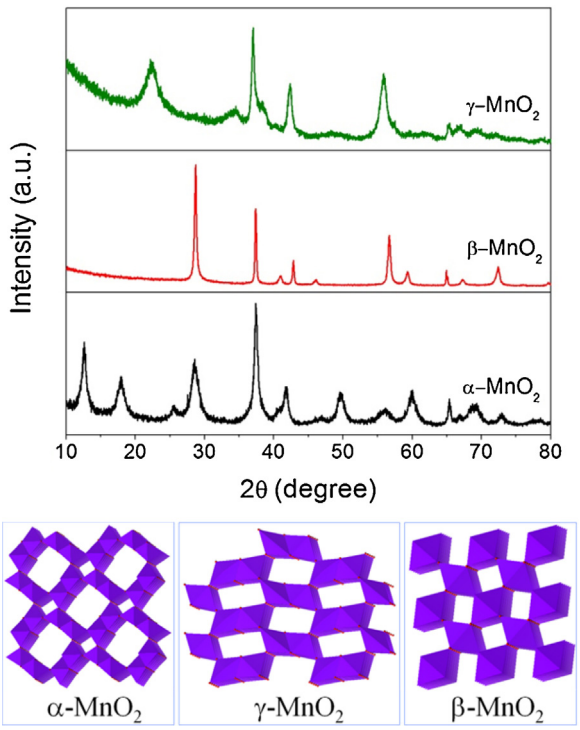

Fig. 1. XRD patterns and crystal structures of α-, β- and γ-MnO_2.

Download English Version:

https://daneshyari.com/en/article/6499183

Download Persian Version:

https://daneshyari.com/article/6499183

Daneshyari.com